Special Section on Clinical Pharmacology

Initial Pharmacological Characterization of a Major Hydroxy Metabolite of PF-5190457: Inverse Agonist Activity of PF-6870961 at the Ghrelin Receptor[S]

Sara L. Deschaine, Morten A. Hedegaard, Claire L. Pince, Mehdi Farokhnia, Jacob E. Moose, Ingrid A. Stock, Sravani Adusumalli, Fatemeh Akhlaghi, James L. Hougland, Agnieszka Sulima, Kenner C. Rice, George F. Koob, Leandro F. Vendruscolo, Birgitte Holst, and Lorenzo Leggio

Clinical Psychoneuroendocrinology and Neuropsychopharmacology Section, Translational Addiction Medicine Branch, National Institute on Drug Abuse Intramural Research Program and National Institute on Alcohol Abuse and Alcoholism Division of Intramural Clinical and Biological Research, National Institutes of Health, Baltimore and Bethesda, Maryland (S.L.D., C.L.P., M.F., L.L.); Department of Pharmacology, University of Michigan Medical School, Ann Arbor, Michigan (S.L.D.); Department of Biomedical Sciences, University of Copenhagen, Copenhagen, Denmark (M.A.H., B.H.); Neurobiology of Addiction Section, Integrative Neuroscience Research Branch, National Institute on Drug Abuse (C.L.P., G.F.K., L.F.V.) and Medication Development Program, National Institute on Drug Abuse Intramural Research Program (A.S., K.C.R., L.L.), National Institutes of Health, Baltimore, Maryland; Department of Mental Health, Johns Hopkins Bloomberg School of Public Health (M.F.) and Division of Addiction Medicine, Department of Medicine, School of Medicine (L.L.), Johns Hopkins University, Baltimore, Maryland; Department of Chemistry (J.E.M., J.L.H.), Department of Biology (J.L.H.), and BioInspired Syracuse (J.L.H.), Syracuse University, Syracuse, New York; Pfizer Inc. Medicine Design, Groton, Connecticut (I.A.S.); Clinical Pharmacokinetics Research Laboratory, Department of Biomedical and Pharmaceutical Sciences, University of Rhode Island, Kingston, Rhode Island (S.A., F.A.); Drug Design and Synthesis Section, Molecular Targets and Medications Discovery Branch, Intramural Research Program, National Institute on Drug Abuse and National Institute on Alcohol Abuse and Alcoholism, National Institutes of Health, Bethesda, Maryland (A.S., K.C.R.); and Center for Alcohol Addiction Studies, Department of Behavioral and Social Sciences, School of Public Health, Brown University, Providence, Rhode Island (L.L.)

ABSTRACT

Preclinical and clinical studies have identified the ghrelin receptor [growth hormone secretagogue receptor (GHSR)1a] as a potential target for treating alcohol use disorder. A recent phase 1a clinical trial of a GHSR1a antagonist/inverse agonist, PF-5190457, in individuals with heavy alcohol drinking identified a previously undetected major hydroxy metabolite of PF-5190457, namely PF-6870961. Here, we further characterized PF-6870961 by screening for off-target interactions in a high-throughput screen and determined its in vitro pharmacodynamic profile at GHSR1a through binding and concentration-response assays. Moreover, we determined whether the metabolite demonstrated an in vivo effect by assessing effects on food intake in male and female rats. We found that PF-6870961 had no off-target interactions and demonstrated both binding affinity and inverse agonist activity at GHSR1a. In comparison with its parent compound, PF-5190457, the metabolite PF-6870961 had lower binding affinity and potency at inhibiting GHSR1a-induced inositol phosphate accumulation. However, PF-6870961 had increased inhibitory potency at GHSR1a-induced β-arrestin recruitment relative to its parent compound. Intraperitoneal

injection of PF-6870961 suppressed food intake under conditions of both food restriction and with ad libitum access to food in male and female rats, demonstrating in vivo activity. The effects of PF-6870961 on food intake were abolished in male and female rats knockout for GHSR, thus demonstrating that its effects on food intake are in fact mediated by the GHSR receptor. Our findings indicate that the newly discovered major hydroxy metabolite of PF-5190457 may contribute to the overall activity of PF-5190457 by demonstrating inhibitory activity at GHSR1a.

SIGNIFICANCE STATEMENT

Antagonists or inverse agonists of the growth hormone secretagogue receptor (GHSR)1a have demonstrated substantial potential as therapeutics for alcohol use disorder. We here expand understanding of the pharmacology of one such GHSR1a inverse agonist, PF-5190457, by studying the safety and pharmacodynamics of its major hydroxy metabolite, PF-6870961. Our data demonstrate biased inverse agonism of PF-6870961 at GHSR1a and provide new structure-activity relationship insight into GHSR1a inverse agonism.

Introduction

Alcohol use disorder (AUD) is a chronic relapsing disease that causes significant harm to an individual's health and is a growing public health concern. However, the number of medications approved to treat AUD remains low, leaving critical need for a broader range of AUD therapeutics. Growing evidence indicates a role of the stomach-derived peptide ghrelin in AUD.

Ghrelin, acylated by ghrelin O-acyltransferase (GOAT) to obtain receptor activity, plays important roles in nutrient sensing and informs homeostatic and hedonic processes regulating appetitive behaviors, including alcohol consummatory behaviors (for reviews, see Yanagi et al., 2018; Deschaine and Leggio, 2022). This role is evidenced by preclinical and clinical studies demonstrating that ghrelin potentiates alcohol seeking and craving (for reviews, see Morris et al., 2018; Farokhnia et al., 2019). In rodents, ghrelin increases alcohol self-administration, alcohol-induced conditioned place preference, and alcohol-induced dopamine release in the nucleus accumbens (Jerlhag et al., 2009). Moreover, antagonism or knockout of the ghrelin receptor [growth hormone secretagogue receptor (GHSR)1a] decreases alcohol self-administration (Kaur and Ryabinin, 2010; Landgren et al., 2012; Suchankova et al., 2013; Morris et al., 2018; Yanagi et al., 2018; Zallar et al., 2019a). In humans, intravenous administration of ghrelin increases self-reported alcohol craving (Leggio et al., 2014), alcohol self-administration, and functional magnetic resonance imaging (fMRI) blood oxygen level–dependent (BOLD) reactivity to alcohol symbols in the amygdala (Farokhnia et al., 2018). Thus, inhibiting the activity of the ghrelin system has been suggested as a potential pharmacotherapy for AUD, which may extend to other substance use disorders as well (for review, see Zallar et al., 2017; You et al., 2022).

The effects of ghrelin on alcohol-related behaviors occur through interaction with its receptor, GHSR1a. GHSR1a is a G-protein-coupled receptor (GPCR) expressed both centrally and peripherally that demonstrates constitutive activity (Holst et al., 2003) and couples to $G\alpha_q$, $G\alpha_{12/13}$, $G\alpha_{i/o}$, and β-arrestin (for review, see Hedegaard and Holst, 2020). We have recently investigated a GHSR1a antagonist/inverse agonist, PF-5190457, as a potential therapeutic for AUD. PF-5190457 is a spiro-azetidino-piperidine compound originally identified and optimized by Pfizer Inc. for GHSR1a inverse agonist/antagonist activity as a potential treatment of type 2 diabetes mellitus (Kung et al., 2012). PF-5190457 displayed inverse agonist/antagonist activity at GHSR1a both in vitro and ex vivo (Kung et al., 2012; Bhattacharya et al., 2014; Kong et al., 2016). Furthermore, PF-5190457 decreased ghrelin-induced growth hormone secretion by 77% and gastric emptying time by 20% in

humans at a dose of 100 mg twice daily, providing indirect evidence of GHSR1a engagement in humans (Denney et al., 2017). Moreover, in a series of rat experiments, followed by a placebo-controlled phase 1b human study with heavy drinking male and female participants, we identified that PF-5190457 (50 mg and 100 mg twice daily) was safe and well tolerated when coadministered with alcohol, had no effects on alcohol metabolism, and showed potential efficacy in behavioral tasks that suggested potential to reduce alcohol and food craving and attention to cues (Lee et al., 2020b).

An unexpected finding from analysis of pooled sera collected during our phase 1b human study was the identification of a major metabolite of PF-5190457 previously unidentified by liquid chromatography–mass spectrometry (LC-MS) of liver microsomal incubations of PF-5190457. Incubating PF-5190457 in liver cytosol reproduced the metabolite observed in our pooled patient sera analysis, suggesting that this metabolite was produced by metabolism of PF-5190457 via liver cytosolic enzymes (Adusumalli et al., 2019a,b). Nuclear magnetic resonance (NMR) spectroscopy analysis of this compound revealed that hydroxy addition occurred on the piperidine group of PF-5190457 to form the metabolite, which was named PF-6870961 (Adusumalli et al., 2019a,b) (Fig. 1). Moreover, liver cytosolic incubation of PF-5190457 with xanthine and aldehyde oxidase inhibitors attenuated production of PF-6870961, suggesting that this metabolite is produced by liver cytosolic xanthine and aldehyde oxidases (Adusumalli et al., 2019b). Because initial screenings of PF-5190457 did not identify PF-6870961 as a major metabolite, the potential on-target/off-target effects of PF-6870961 and resulting implications for the overall safety and efficacy of PF-5190457 were unknown. Therefore, we conducted a series of experiments to determine the characteristics of PF-6870961 and further understand the pharmacological profile of PF-5190457. We assessed whether PF-5190457 and/or PF-6870961 alter ghrelin acylation by inhibiting GOAT activity and compared the in vitro activity at GHSR1a of PF-5190457, PF-6870961, and the recently discovered endogenous GHSR1a antagonist, liver-expressed antimicrobial peptide 2 (LEAP-2) (Ge et al., 2018).

Methods

PF-5190457 and PF-6870961 Compounds

In our placebo-controlled phase 1b human study (Lee et al., 2020b), participants were administered PF-5190457 (molecular mass = 512 Da) provided in kind by Pfizer Inc. (New York, NY). For GHSR1a binding affinity studies, PF-5190457 was obtained from a Pfizer-provided stock, and PF-6870961 (molecular mass = 528 Da) was synthesized at the National Institute on Drug Abuse (NIDA) Intramural Research Program using a modified synthetic route to the previously published synthetic route for PF-5190457 (Bhattacharya et al., 2014). The metabolite was produced on a gram sale with an overall 55% yield starting from (1R)-5-bromoindanam; for a detailed description of the synthesis of PF-6870961, please see Sulima

ABBREVIATIONS: AUD, alcohol use disorder; BRET, bioluminescent resonance energy transfer; CI, confidence interval; CoA, coenzyme A; CR1, neutral cue reactivity; CR2, food cue reactivity; CR3, alcohol cue reactivity; ECL, extracellular loop; GFCQ-S, General Food Craving Questionnaire–State; GHSR, growth hormone secretagogue receptor; GOAT, ghrelin O-acyltransferase; GPCR, G-protein–coupled receptor; HEK, human embryonic kidney; hGOAT, human ghrelin O-acyltransferase; HPE, hundred percent effect; IP, inositol phosphate; K_i, inhibition constant; KO, knockout; LEAP-2, liver-expressed antimicrobial peptide 2; NIAAA, National Institute on Alcohol Abuse and Alcoholism; NIDA, National Institute on Drug Abuse; T1, predose timepoint; T2, postdose timepoint; TMD, transmembrane domain; ZPE, zero percent effect.
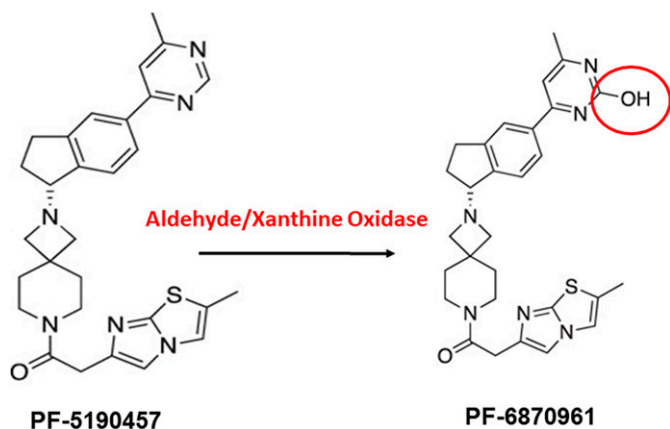
Fig. 1. Structure of PF-5190457 and PF-6870961. PF-5190457 is converted to PF-6870961 through the addition of a hydroxy group to the piperidine ring. This reaction occurs via cytosolic enzymes, namely xanthine and aldehyde oxidases.

et al. (2021). For GOAT and GHSR1a inhibition experiments, PF-5190457 was purchased from Sigma Aldrich (≥95% purity, PZ0270; St. Louis, MO) and PF-6870961 was synthesized at NIDA Intramural Research Program (Sulima et al., 2021). Rodent experiments used a second batch of PF-6870961 synthesized as a hydrochloride salt for improved solubility as described in Sulima et al. (2021).

High-Throughput Screen of PF-6870961

To evaluate off-target effects of the hydroxy metabolite, PF-6870961 was dissolved in 0.1% dimethyl sulfoxide (DMSO) and evaluated across 71 binding and enzyme targets at concentrations of 100 nM and 10,000 nM (Eurofins Cerep, Le Bois-l'Évêque, France). Each experiment was performed in duplicate. Compound binding was calculated as percent binding inhibition of a radioactively labeled ligand specific for each target. Compound enzyme inhibition was calculated as percent inhibition of control enzymatic activity. More than 50% binding or enzyme inhibition was considered a significant effect of PF-6870961 at the target.

A separate screen was conducted for serotonin, dopamine, and opioid receptors, as well as biogenic amine transporters, for a total of 13 additional targets (VA Medical Center R&D, Portland, OR). Interaction of PF-6870961 dissolved in 0.1% DMSO with these targets was evaluated at concentrations of 100 nM and 10,000 nM for inhibition of a radioligand specific for each target. For this screen, each target was evaluated in triplicate and experiments were repeated at least twice. Nonspecific binding was subtracted from all data, and specific binding in the presence of drug was normalized to specific binding in the absence of drug.

GOAT Activity Assay with PF-5190457 and PF-6870961

Methyl arachidonyl fluorophosphonate (MAFP; Cayman Chemical, Ann Arbor, MI) was diluted in DMSO from a stock in methyl acetate. Octanoyl coenzyme A (octanoyl CoA; CoALA, Austin, TX) was diluted to 5 mM in 10 mM Tris-HCl pH 7.0 and stored in low adhesion tubes at −80°C until use. The ghrelin-mimetic GSSFLC$_{NH2}$ peptide substrate was commercially synthesized by Sigma-Genosys (The Woodlands, TX) in PEPscreen format. The GSSFLC$_{NH2}$ peptide was solubilized

in 1:1 acetonitrile/water solution and stored at −80°C. Peptide concentration was determined spectrophotometrically at 412 nm by reaction of the cysteine thiol with 5,5′dithiobis (2-nitrobenzoic acid) using an ϵ_{412} of 14,150 M^{-1} cm^{-1} (Riddles et al., 1979). Peptide substrates were fluorescently labeled with acrylodan and purified via reverse phase high-performance liquid chromatography (HPLC) as previously reported (Darling et al., 2015; Sieburg et al., 2019). Human GOAT (hGOAT) was expressed and enriched in insect (Sf9) membrane protein fractions using a previously published procedure (Darling et al., 2015; McGovern-Gooch et al., 2017; Sieburg et al., 2019). Membrane protein fractions from Sf9 cells expressing hGOAT were thawed on ice and then homogenized by passage through an 18-gauge needle 10 times. Assays were performed with 10 μg of membrane protein as determined by Bradford assay. For each set of 10 samples, a 440-μl master mix was prepared containing 2.5 mM N-2-hydroxyethylpiperazine-N-2-ethane sulfonic acid (HEPES), 10 μM methyl arachidonyl fluorophosphonate (MAFP), and 110 μg membrane protein. Forty microliters of the master mix was aliquoted into each low-adhesion microcentrifuge tube. Compounds PF-6870961 and the previously reported GOAT inhibitor, NSM-48, were diluted in DMSO to concentrations of 0.5 mM, 5.0 mM, and 50 mM prior to addition to the reaction mixture (McGovern-Gooch et al., 2017). Due to solubility limitations, compound PF-5190457 was solubilized in DMSO to concentrations of 0.1 mM, 1.0 mM, and 1.95 mM prior to addition to the reaction mixture. One microliter of inhibitor stock and 4 μl DMSO (5 μl of PF-5190457 stocks) were added to each reaction and allowed to preincubate for 30 minutes at room temperature. Reactions were initiated by the addition of octanoyl CoA (300 μM final concentration) and GSSFLC$_{AcDan}$ peptide (1.5 μM final concentration) to yield a final reaction volume of 50 μl. Reactions were incubated for 30 minutes at room temperature while sealed and then stopped by addition of 50 μl of 20% acetic acid in isopropanol. Membrane proteins were then removed via precipitation with 16.7 μl of 20% trichloroacetic acid followed by centrifugation (1000 × g, 1 minute). The supernatant was analyzed via reverse-phase HPLC as previously described (Sieburg et al., 2019). GOAT acylation activity was determined by substrate and product peak integration in the presence of either sample or vehicle (DMSO). Percent activity was calculated using eq. 1 and eq. 2 below:

$$\% \text{ activity} = \frac{\% \text{ peptide octanoylation in presence of inhibitor}}{\% \text{ peptide octanoylation in absence of inhibitor}} \quad (1)$$

$$\% \text{ peptide octanoylation} = \frac{\text{fluorescence of octanoylated peptide}}{\text{total peptide fluorescence}} \quad (2)$$

GHSR1a Membrane Filter Binding Assay (Human, Rat, and Dog)

Ghrelin binding assays were performed in 96-well plates in a final volume of 100 μl containing 250 ng (human or rat) or 2 mg (dog) GHSR1a [from human embryonic kidney (HEK)293 tetracycline-inducible cell lines expressing GHSR1a; prepared as membranes] and 50 pM [^{125}I] ghrelin (NEX-388; PerkinElmer Life Sciences, Waltham, MA), plus varying concentrations of test compound or vehicle. Zero percent effect (ZPE) was defined by blank controls included on each plate, and 100% effect (HPE) was defined by wells where 1 mM

unlabeled ghrelin was added to maximally displace the radioligand. All reagents were diluted in assay buffer [50 mM HEPES, 10 mM $MgCl_2$, 0.2% bovine serum albumin (BSA), ethylenediaminetetraacetic acid (EDTA)-free protease inhibitors mix, pH 7.4], and reactions were incubated for 90 minutes at room temperature to allow binding to reach equilibrium. The reactions were transferred to a 0.3% polyethyleneimine (PEI)-treated, 96-well glass fiber filtration plate (6005174; PerkinElmer) and washed three times with ice-cold 50 mM Tris, pH 7.5 by vacuum filtration. Plates were allowed to dry overnight at room temperature, and the amount of receptor-ligand complex was determined by liquid scintillation counting using a 1450 MicroBeta TriLux (Wallac, Victoria, Australia). Data analysis was performed using a proprietary software package. Briefly, the percent effect for each compound dose (Sample) was calculated from raw data as follows: % effect = 100-100 × ((Sample-HPE)/(ZPE − HPE)), where HPE and ZPE values are averages of four wells each. The compound percent effect values were then plotted versus log compound concentration, and the inhibition constant (K_i) was determined as follows: $K_i = IC_{50}/(1 + ([radioligand]/K_d))$, where the IC_{50} was determined from a standard 4-parameter fit algorithm and the dissociation constant (K_d) value was specific to the batch of GHSR1a membranes used in the assay.

GHSR1a Inhibition Assays with PF-5190457, PF-6870961, and LEAP-2

Inositol phosphate (IP) turnover assay: COS-7 cells (ATCC CRL-1651) were cultured in Dulbecco's modified Eagle's medium (DMEM) 1885 supplemented with 10% fetal bovine serum (FBS), 1% penicillin/streptomycin, and 2 mM L-glutamine at 37°C in a 10% CO_2 incubator. The cells were seeded at a density of 20,000 cells per well in a 96-well plate and allowed to attach overnight. Cells were then transfected by chloroquine-induced calcium precipitation with pCMV-Tag2B plasmid (Stratagene, La Jolla, CA) containing GHSR–wild-type (WT) at a concentration of 0.4 μg DNA per well. The GHSR-WT construct was generated by polymerase chain reaction (PCR) overlap extension with Pfu polymerase (Promega, Madison, WI) as previously described (Mokrosiński et al., 2012) and verified by DNA sequencing (Eurofins MWG Operon, Huntsville, AL). After 5 hours, the transfection medium was changed to the cultivation medium [μl/ml of Myo-[2-3H(N)]-inositol (PerkinElmer)] and the cells were incubated for 2 days at 37°C in a 10% CO_2 incubator.

Prior to IP accumulation studies, the cells were washed once with 37°C 1× Hank's Balanced Salt Solution (HBSS) buffer. After washing, the cells were incubated at 37°C with 100 μl 37°C 1× HBSS buffer containing 10 mM lithium chloride (LiCl) and the appropriate ligand [ghrelin (Polypeptide Inc., Hillerød, Denmark), LEAP-2 (Peptide Institute Inc., Japan), PF-5190457, or PF-6870961] at different concentrations for 90 minutes. After incubation, the plates were placed on ice and the cells were lysed with ice-cold 10 mM formic acid for at least 30 minutes. After lysing, the cells were transferred to a white-bottomed 96-well plate containing scintillation proximity assay yttrium silicate (SPA-YSI) beads (PerkinElmer). Plates were shaken at maximum speed on a plate shaker for a minimum of 10 minutes at room temperature, after which the plates were spun at 1500 rpm for 5 minutes and incubated at room temperature for 4 hours prior to measurement. The

measurements were performed on a MicroBeta plate reader (PerkinElmer) with a 3-minute measuring time. The experiment was completed independently in triplicate.

β-Arrestin Recruitment Assay. The bioluminescence resonance energy transfer (BRET) experiments were carried out as previously described (Spiess et al., 2019). Briefly, 24 hours after seeding cells in a 6-well plate, 60%–80% confluent HEK293 cells were transfected with the following plasmids: GHS-R1a, empty pcDNA3.1(+) vector (negative control), or human glucagon-like peptide-1 receptor (GLP-1R, positive control) in combination with the BRET donors (renilla luciferase–fused arrestins, RLuc8–arrestin-2–Sp1 or RLuc8–arrestin-3–Sp1), the BRET acceptor mem-linker-citrine-SH3 (SRC homology 3 domain), and GPCR kinase 2 (GRK2) to facilitate β-arrestin-1 and β-arrestin-2 recruitment. After 24 hours, the cells were washed with phosphate-buffered saline (PBS) and resuspended in PBS with 5 mmol/l glucose. Eighty-five microliters of cell suspension was added to each well on a 96-well isoplate followed by the addition of PBS with 5 μmol/l coelenterazine h (final concentration). After 10 minutes at room temperature, increasing concentrations of glucagon-like peptide 1 (GLP-1) were added to the positive control cells. Luminescence was measured with an EnVision plate reader (PerkinElmer) [RLuc8 at 485 ± 40 nm and yellow fluorescent protein (YFP) at 530 ± 25 nm]. The experiment was completed independently in triplicate.

2.6 Food and Locomotor Assays with PF-5190457 and PF-6870961 in Rats

Animals. Adult male ($n = 15$) and female ($n = 15$) Wistar rats were purchased from Charles River (Raleigh, NC) and were 8 weeks old at the beginning of the experiments. The GHSR knockout (KO) Wistar rats were bred at the NIDA Intramural Research Program (NIDA-IRP) using heterozygous animals. Rats were single housed and held in temperature- and humidity-controlled rooms on a reverse 12-hour/12-hour light/dark cycle (lights off at 7:00 a.m.) and had ad libitum access to food and water except during food intake experiments. All procedures were performed accordingly to National Institutes of Health *Guide for the Care and Use of Laboratory Animals* and were approved by the Institutional Animal Care and Use Committee of the NIDA Intramural Research Program.

Food Intake. Rats were split into two drug treatment groups: PF-5190457 and PF-6870961. Treatment groups were matched by body weight (kg) and sex (five males and five females per group). PF-5190457 was prepared with a few drops of Tween 80 and diluted with saline to yield doses of 5 mg/kg, 10 mg/kg, and 15 mg/kg. PF-6870961 was prepared in the same manner with doses of 2.5 mg/kg, 10 mg/kg, and 40 mg/kg, which were selected based on our observations in humans that plasma concentrations of PF-6870961 were ∼25% of PF-5190457 plasma concentrations. Vehicle (0 mg/kg) was prepared with 4% Tween 80 and saline. As a positive control, a third group ($n = 10$; 5 males, 5 females) was treated with 10 mg/kg of the widely used prototype GHSR1a antagonist, JMV2959 (Sigma Aldrich). This dose was selected based on previous studies demonstrating reductions in food intake at even lower doses of JMV2959 (Moulin et al., 2013; Gomez and Ryabinin, 2014). JMV2959 was diluted with saline, and saline served as the vehicle. The injection volume for all drugs was 3 ml/kg body weight. Drug administration was intraperitoneal

immediately prior to testing. Following a within-subjects, Latin-square design, rats were given intraperitoneal injections of PF-5190457 or PF-6870961 according to group assignment. In the third cohort, 10 mg/kg JMV2959 and vehicle were administered in a counterbalanced manner. Chow was weighed to the nearest 0.1 g immediately prior to injection and 1 hour later. In the satiated condition, rats had ad libitum access to standard chow. In the fasted condition, chow was removed for 18 hours prior to drug treatment. Drug administrations were separated by at least 24 hours. To verify that any observed effects of PF-6870961 were mediated via GHSR1a, an additional experiment was conducted later on to again assess food intake in both fed and fasted conditions after administration of either vehicle or the highest dose of PF-6870961 (40 mg/kg) using a within-subjects design in age-matched (8 weeks) male and female GHSR KO Wistar rats. This transgenic CRISPR/Cas9 line of GHSR KO rats was previously developed at the NIDA Intramural Research Program (Zallar et al., 2019b).

Spontaneous Locomotion. PF-5190457 was prepared as described above. Due to limited availability of PF-6870961, only the effect of PF-5190457 (30 mg/kg) on spontaneous locomotion was assessed using an open field test. Rats ($n = 10$; 5 males, 5 females) were first habituated to the apparatus with gray floor and plexiglass walls (40 cm × 40 cm) for 15 minutes. The next day, rats were administered vehicle or 30 mg/kg PF-5190457 in a randomized order, and were put in the center of the open field 30 minutes post-administration. Locomotion was recorded for 15 minutes. One day later, all rats were tested again for locomotion with the opposite vehicle or PF-5190457 treatment of test 1. Open field tests were conducted in a room with red light. ANY-maze Video Tracking software (Global Biotech, Mount Laurel, NJ) was used to track total distance traveled (m) and average speed (m/s) of each rat.

Statistical Analysis. Significant outliers were identified using the ROUT method (Q = 1%) and excluded. For food intake experiments, one-way analysis of variance (ANOVA) was used to analyze an effect of dose for PF-5190457– and PF-6870961–treated rats. Paired Student's *t* test was used to assess the effect of dose on food intake in JMV2959-treated animals. For spontaneous locomotion, a paired Student's *t* test was used to compare PF-5190457 treatment to vehicle. In the case of outlier exclusion, mixed-effects analyses were performed in lieu of ANOVA. If a main effect of treatment was observed, Dunnett post hoc tests were used to determine the significant difference(s). GraphPad Prism Software (San Diego, CA) was used for statistical analyses.

Analysis of PF-6870961 and PF-5190457 Concentration in Humans

We evaluated the concentration of PF-6870961 in plasma samples of all participants enrolled in our parent phase 1b human study of PF-5190457, whose main results have been published elsewhere (Lee et al., 2020b). Briefly, participants were recruited to the National Institute on Alcohol Abuse and Alcoholism (NIAAA) inpatient unit at the National Institutes of Health (NIH) Clinical Center in Bethesda, Maryland, through flyers and advertisements. Potential candidates underwent a phone screen before completing an in-person screen during

which a battery of assessments and clinical laboratories was performed. Male and female participants meeting inclusion criteria consumed >14 and 7 drinks a week, respectively, according to Timeline Followback data. A full description of inclusion and exclusion criteria has been published (Lee et al., 2020b) and can also be found in Supplemental Appendix 1. The human phase 1b study was approved by the appropriate Institutional Review Board and conducted under the US Food and Drug Administration (FDA) Investigational New Drug 119,365. Each participant provided written informed consent before being enrolled. The study had a within-subject, placebo-controlled, single escalating dose design where patients participated to three separate 3-day visits (separated by proper between-visit washout periods). During each 3-day visit, PF-5190457 was given five times to reach steady state. Specifically, participants received placebo at the first 3-day visit, 50 mg twice daily PF-5190457 at the second 3-day visit, and finally 100 mg twice daily PF-5190457 at the third 3-day visit. Blood samples were collected in the early (8:00 a.m.) and late (10:45 a.m.) morning and afternoon of the first 2 days of each visit. On the third day, multiple blood samples were collected after consumption of a standardized oral alcohol beverage to observe any possible interaction between PF-5190457 and alcohol. Blood was immediately centrifuged at 1700 × g for 15 minutes at 4°C, and extracted plasma was stored at −80°C until analysis. The concentrations of PF-5190457 and PF-6870961 were determined using a previously published liquid chromatography–mass spectrometry (LC-MS) method (Adusumalli et al., 2019a).

Correlation analyses between self-reported food craving scores and plasma concentrations of PF-5190457 and PF-6870961 were conducted using self-report data and blood samples collected on the first and second day of visit 3, where participants received 100 mg twice daily of PF-5190457. Briefly, for the first 2 days of a visit, the General Food Craving Questionnaire–State (GFCQ-S) was given before (8:30 a.m.) and after (10:00 a.m.) the morning dose of placebo or PF-5190457. On the second day of each visit, a cue reactivity procedure was performed in a bar-like environment in which participants were administered the GFCQ-S after exposure to neutral cues, food-related cues, and alcohol-related cues. Full details and main findings of this procedure have been previously published (Lee et al., 2020b). Participants provided information regarding their preferred snack or alcohol beverage at the beginning of the study, and these choices served as the food and alcohol cues used during the experiment. To evaluate any preliminary relationship between PF-6870961 or PF-5190457 and food craving, Pearson correlations were calculated between individual metabolite or parent compound concentrations and GFCQ-S scores were collected on the first and second days of the last visit (where participants received 100 mg twice daily PF-5190457) using SPSS (IBM, Armonk, NY). Specifically, correlation scores were calculated between the change in GFCQ-S score (postdose or T2 − predose or T1) and the change in PF-6870961 or PF-5190457 concentration (T2 − T1) on both day 1 and day 2 concentration and GFCQ-S scores collected during alcohol cue reactivity after neutral (CR1), food (CR2), and alcohol (CR3) sensory and olfactory cues were calculated. Scatterplots of PF-5190457 and PF-6870961 plasma concentration and GFCQ-S scores were generated in R version 4.1.2 (R Core Team, 2022).

Results

PF-6870961 Has No Off-Target Effects in a High-Throughput Screen

PF-6870961 did not produce greater than 50% inhibition of radioligand binding or control enzymatic activity for all targets tested at both concentrations of 0.1 μM and 10 μM (Supplemental Table 1). Highest inhibition effects were observed for 10,000 nM PF-6870961 at dopamine receptor 4.4 (D4.4) and choline acetyl transferase, producing 43.5% and 46.4% inhibition, respectively. Additionally, PF-6870961 did not produce greater than 50% inhibition of radioligand binding at either concentration tested of 0.1 μM and 10 μM for dopamine, opioid, and serotonin receptors and dopamine, serotonin, and norepinephrine transporters (Supplemental Table 2).

PF-5190457 and PF-6870961 Do Not Inhibit GOAT Activity

To determine whether PF-5190457 and PF-6870961 could interfere with the activity of GOAT, the enzyme that acylates ghrelin, PF-5190457 and PF-6870961 were tested for potential hGOAT inhibitory activity. PF-5190457 was limited in testing due to poor solubility and did not appreciably inhibit hGOAT at the highest tested concentration ($\sim$30% inhibition at 195 μM), exhibiting no evidence for concentration-dependent inhibition. PF-6870961 also did not inhibit hGOAT, with less than 20% inhibition at 1000 μM. (Fig. 2).

PF-6870961 Binds to GHSR1a with Lower Affinity Than PF-5190457

PF-5190457 and PF-680961 binding affinity to GHSR1a was determined in three species (human, rat, and dog) in a competitive binding assay using [I^{125}] ghrelin as a radioligand (Table 1). For PF-6870961, mean K_i values for human ($n = 6$), rat ($n = 6$), and dog ($n = 6$) GHSR1a were 73.6 nM [95% confidence interval (CI): 52.4–103 nM], 239 nM (95% CI: 218–262 nM), and 217 nM (95% CI: 186–253 nM), respectively. For PF-5190457, K_i values calculated from experiments with human ($n = 3$), rat ($n = 3$), and dog ($n = 3$) GHSR1a were 2.96 nM (95% CI: 2.64–3.33 nM), 3.94 nM (95% CI: 2.88–5.39 nM), and 4.88 nM (95% CI: 4.23–5.64 nM), respectively. Data for PF-5190457 were not significantly different from previous

data collected by Pfizer on GHSR1a binding affinity (human: $n = 52$, $K_i = 2.49$ nM; rat: $n = 49$, $K_i = 3.19$ nM; dog: $n = 9$, $K_i = 3.56$ nM). Overall, PF-6870961 had approximately 25-, 60-, and 44-fold lower affinity than PF-5190457 for human, rat, and dog GHSR, respectively.

PF-6870961 Displays Inverse Agonist Activity at GHSR1a

PF-6870961 inhibited the constitutive GHSR1a-induced IP accumulation with an IC_{50} value of 300 nM. This was a higher effective concentration than either PF-5190457 or LEAP-2 (the endogenous agonist of GHSR1a), which inhibited constitutive GHSR1a-induced IP mobilization at IC_{50} values of 6.8 nM and 4.7 nM, respectively, suggesting approximately 50-fold lower potency of PF-6870961 at GHSR1a (Fig. 3, A and B; Table 2). However, in the case of GHSR1a-induced β-arrestin mobilization, PF-6870961 had higher inhibitory potency than PF-5190457 and LEAP-2, with an IC_{50} of 1.1 nM for inhibition of GHSR1a constitutive activity (Fig. 3, C and D; Table 2). Constitutive GHSR1a β-arrestin mobilization was inhibited by LEAP-2 with an IC_{50} of 20.5 nM and by PF-5190457 with an IC_{50} of 3.4 nM.

Both PF-5190457 and PF-6870961 Suppress Food Intake in Male and Female Rats

Initial analyses of the data identified no significant main effect of sex on food intake in each treatment group; therefore, the analysis was simplified to either mixed-effects analysis or one-way ANOVA depending on the presence of outliers in the sample. Mixed-effects analysis indicated a significant effect of PF-5190457 on food intake (g chow/kg body weight) in satiated male and female rats ($F_{4,34} = 3.236$, $P = 0.0236$), and post hoc analyses showed that PF-5190457 significantly reduced food intake at 30 mg/kg ($P = 0.0118$) compared with vehicle (Fig. 4A). Outlier data from two female rats at the 30 mg/kg dose were not included in the analysis. One-way ANOVA showed a significant effect of PF-5190457 on food intake in fasted male and female rats ($F_{4,36} = 2.705$, $P = 0.0455$). PF-5190457 significantly reduced food intake at 30 mg/kg ($P = 0.0222$) compared with vehicle (Fig. 4B). Mixed-effects analysis indicated a significant effect of PF-6870961 on food intake in satiated male and female rats ($F_{3,34} = 3.372$, $P = 0.0295$).
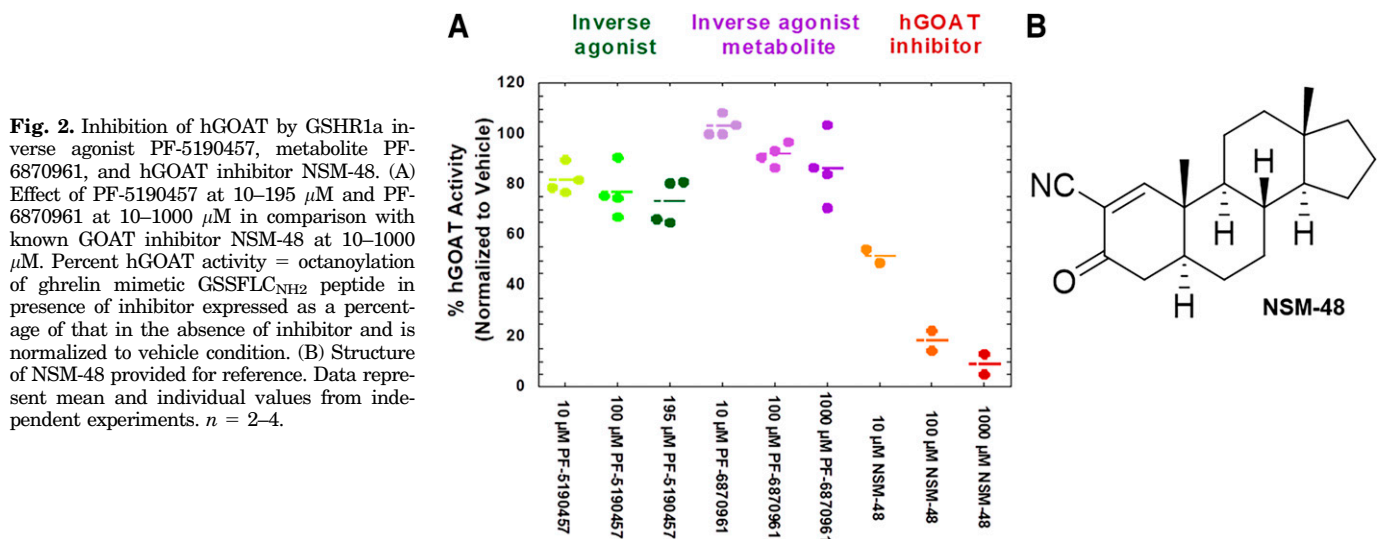
Fig. 2. Inhibition of hGOAT by GSHR1a inverse agonist PF-5190457, metabolite PF-6870961, and hGOAT inhibitor NSM-48. (A) Effect of PF-5190457 at 10–195 μM and PF-6870961 at 10–1000 μM in comparison with known GOAT inhibitor NSM-48 at 10–1000 μM. Percent hGOAT activity = octanoylation of ghrelin mimetic GSSFLC$_{NH2}$ peptide in presence of inhibitor expressed as a percentage of that in the absence of inhibitor and is normalized to vehicle condition. (B) Structure of NSM-48 provided for reference. Data represent mean and individual values from independent experiments. $n = 2$–4.

TABLE 1
Binding affinity of PF-5190457 and PF-6870961 to GHSR

	Hill Slope	K_i (nM)	95% CI Lower Limit (nM)	95% CI Upper Limit (nM)
PF-5190457				
Human GHSR	1.061	2.96	2.64	3.33
Rat GHSR	0.947	3.94	2.88	5.39
Dog GHSR	1.251	4.88	4.23	5.64
PF-6870961				
Human GHSR	0.789	73.6	52.4	103
Rat GHSR	0.811	239	218	262
Dog GHSR	0.929	217	186	253

PF-6870961 significantly reduced food intake at 40 mg/kg versus vehicle (P = 0.0130; Fig. 4C). Outlier data from two female rats at the 40 mg/kg dose were not included in the analysis. Likewise, PF-6870961 significantly reduced food intake in fasted male and female rats ($F_{3,27}$ = 11.22, P < 0.0001). PF-6870961 significantly reduced food intake at 40 mg/kg versus vehicle (P = 0.0053; Fig. 4D). As a positive control, the GHSR1a antagonist, JMV2959, was also tested. A paired t test showed a significant effect of 10 mg/kg JMV2959 versus vehicle on food intake in the satiated condition (t_9 = 2.975, P = 0.0156; Fig. 4E). However, no significant difference was observed for the fasted condition (t_9 = 0.4673, P = 0.6514; Fig. 4F). In GHSR KO rats, paired t test identified no significant difference between vehicle- or PF-6870961 (40 mg/kg i.p.)–treated groups on food intake in either satiated (t_9 = 0.2442, P = 0.81) or fasted (t_9 = 1.586, P = 0.15) conditions (Fig. 5). A paired t test showed no significant effect of PF-5190457 on distance traveled (t_9 = 0.4088, P = 0.692; Supplemental Fig. 1A) or average speed (t_9 = 0.4182, P = 0.686; Supplemental Fig. 1B) in the open field.

Correlation between PF-5190457 and PF-6870961 Concentration and Food Craving in Humans

Demographics for the sample are included in Table 3. Average plasma concentrations of PF-5190457 and PF-6870961 for each of the three visits of our phase 1b study indicated that the metabolite circulated at a concentration approximately 25% of the concentration of the parent compound (Fig. 6; Supplemental Table 3). Pearson correlations between GFCQ-S scores and plasma concentrations of PF-5190457 and PF-6870961 revealed no correlation between parent or metabolite plasma concentration and self-reported food craving indexed by GFCQ-S (Fig. 7; Table 4).

Discussion

We report the initial pharmacological characterization of PF-6870961, a new major metabolite of PF-5190457 that we recently discovered. Here we demonstrated that PF-6870961 exhibits no off-target activity in a full high-throughput screen of binding and enzymatic targets. We have demonstrated that PF-6870961 binds to human GHSR1a with approximately 25-fold lower affinity than PF-5190457 and displays inverse agonist at GHSR1a by inhibiting both constitutive GHSR1a activity. Both PF-5190457 and PF-6870961 did not inhibit GOAT enzymatic activity, indicating that both the parent and metabolite compounds do not suppress ghrelin acylation. Lastly, we identified that both parent and metabolite compounds significantly suppress food intake in male and female rats in fed and fasted states.

The GHSR1a is a member of the class B family of 7 transmembrane domain (TMD) GPCRs. Recent structural insight into the binding mechanism of PF-5190457 at GHSR1a indicates that the (6-methylpyrimidin-4-yl)-2,3-dihydro-1 H-inden-1-yl moiety (hydroxylated in PF-6870961) gets pushed into the cleft between TMD2 and TMD3, where it forms hydrophobic and van der Waals interactions with surrounding residues (Qin et al., 2022). Our observation that PF-6870961 had approximately 25-fold lower affinity for human GHSR1a in a competitive binding assay could therefore be due to the increased polarity of this moiety introduced by the hydroxyl group in a binding pocket, where hydrophobic interactions between the receptor and parent compound are observed. Consistent with our observations of lower affinity, PF-6870961
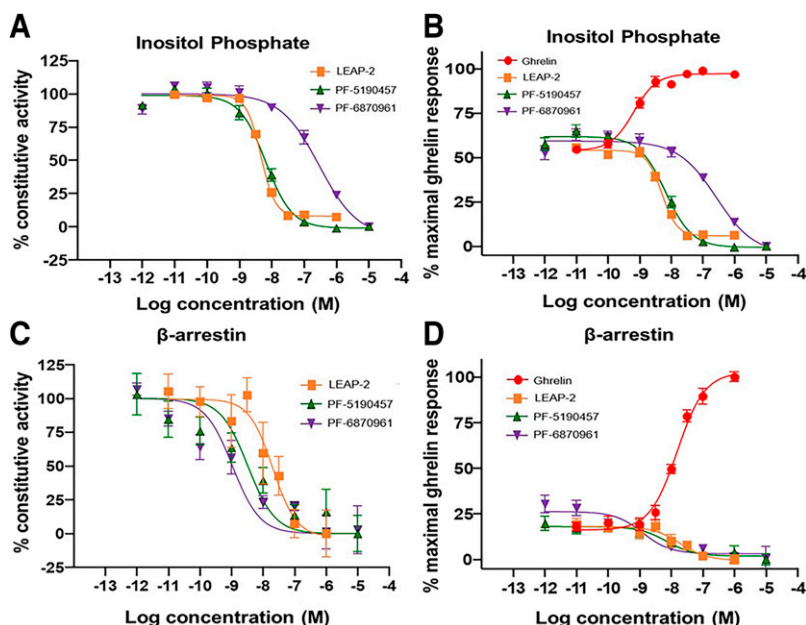

Fig. 3. Inhibition of GHSR1a-induced IP mobilization and β-arrestin mobilization by PF-5190457, PF-6870961, and LEAP-2. Concentration response assay to assess inhibitory potency of compounds at GHSR1a expressed on HEK293 cells (A) Inhibition of constitutive GHSR1a inositol phosphate (IP) mobilization in the presence of increasing concentrations of PF-5190457, PF-6870961, or LEAP-2. (B) Inhibition of GHSR1a IP mobilization as a percentage of the maximal ghrelin-induced response in the presence of increasing concentrations of PF-5190457, PF-6870961, or LEAP-2. (C) Inhibition of constitutive GHSR1a β-arrestin recruitment in the presence of increasing concentrations of PF-5190457, PF-6870961, or LEAP-2. (D) Inhibition of GHSR1a β-arrestin recruitment as a percentage of the maximal ghrelin-induced response in the presence of increasing concentrations of PF-5190457, PF-6870961, or LEAP-2. Data represent mean ± S.E.M. n = 3. β-arrestin = β-arrestin 1 and β-arrestin 2.

TABLE 2
Inhibition of GHSR1a-induced IP and β-arrestin mobilization by LEAP-2, PF-5190457, and PF-6870961

|	Normalized to Constitutive GHSR1a Activity			Normalized to 100% Ghrelin-Induced Activity			
	LEAP-2	PF-5190457	PF-6870961	Ghrelin	LEAP-2	PF-5190457	PF-6870961
IP							
Bottom	7.738	−0.93520	−7.797	53.95	5.869	−0.6585	−4.356
Top	98.81	98.61	100.1	97.09	54.17	61.78	59.26
Hill Slope	−1.966	−1.073	−0.7264	1.192	−1.795	−1.039	−0.7219
EC$_{50}$ (M)	—	—	—	6.58×10^{-10}	—	—	—
IC$_{50}$ (M)	4.77×10^{-9}	6.76×10^{-9}	3.01×10^{-7}	—	5.14×10^{-9}	6.87×10^{-9}	2.752×10^{-7}
Span	91.07	99.54	107.9	43.14	48.30	62.44	63.62
β-Arrestin							
Bottom	−2.582	0.000	0.000	16.12	17.97	17.91	26.20
Top	99.65	100.0	100.0	102.5	−0.5703	1.769	3.128
Hill Slope	−1.154	−1.000	−1.000	1.00	−1.00	−1.00	−1.00
EC$_{50}$ (M)	—	—	—	1.56×10^{-8}	—	—	—
IC$_{50}$ (M)	2.05×10^{-8}	3.39×10^{-9}	1.10×10^{-9}	—	1.98×10^{-8}	7.23×10^{-9}	1.26×10^{-9}
Span	102.2	100.0	100.0	86.40	−18.54	−16.14	−23.07

—, not applicable.

demonstrated less inverse agonism of GHSR1a-stimulated production of IP. GHSR1a couples to Gα_q proteins, which activate phospholipase C (PLC) to stimulate the production of inositol 3,4,5 triphosphate (IP$_3$) among other downstream effects. To assess inhibitory potency at GHSR1a, we evaluated the ability of both PF-5190457 and PF-6870961 to inhibit constitutive Gα_q-stimulated production of IP via GHSR1a. PF-6870961 demonstrated 50-fold lower potency at inhibiting constitutive GHSR1a induction of IP, which was not unexpected, due to its lower binding affinity for the receptor. In comparison with the endogenous antagonist of GHSR1a, LEAP-2, PF-5190457 had similar potency against constitutive IP production. It has been shown that alanine substitution for F119 and Q120 (residues that interact with the PF-5190457 moiety that is hydroxylated on the metabolite) significantly reduce inhibition of GHSR1a-stimulated IP$_1$ accumulation via PF-5190457 (Qin et al., 2022). This raises the possibility that the introduction of a polar group in this pocket may disrupt hydrophobic interactions with F119 and Q110 necessary for inverse agonism of Gα_q-stimulated pathways. Still, we found that in the case of GHSR1a activation of Gα_q, PF-6870961 is a weak inverse agonist, and that PF-5190457 displays similar potency to LEAP-2.

GHSR1a has been shown to not only couple to Gα_q but also to G$\alpha_{i/o}$, G$_{12/13}$, and β-arrestin proteins (Hedegaard and Holst, 2020). To assess the inhibitory potency of our parent and metabolite compound at a different signaling pathway downstream of GHSR1a, we again compared the effective inhibitory concentrations of PF-5190457, PF-6870961, and LEAP-2 (the latter being a recently discovered endogenous antagonist of GHSR1a) in the case of constitutive and ghrelin-induced GHSR1a recruitment of β-arrestin (Ge et al., 2018). We found that PF-6870961 had the lowest effective concentration for both constitutive GHSR1a recruitment of β-arrestin, displaying approximately 20-fold higher potency than LEAP-2 and slightly higher potency (4- to 7-fold) than PF-5190457. The equivalent potency of the metabolite to the parent compound was unexpected given the lower affinity and thus lower occupancy of the receptor expected at similar concentrations to the parent compound. β-Arrestin recruitment to GPCRs occurs through phosphorylation of serine and threonine residues on the C-terminal tail of the active receptor through G-protein—coupled receptor kinases (GRKs). The constitutive activity of GPCRs (including constitutive β-arrestin recruitment) often involves conformational flexibility that allows outward movement of TMD5 relative to TMD3, which permits association with the Gα subunit via interactions with the 7 TMD barrel on the intracellular side. This has also been found to be important for constitutive activity of GHSR1a, as mutations disrupting extracellular loop (ECL)2 flexibility (normally allowing

Fig. 4. Effect of PF-5190457, PF-6870961, and JMV2959 on food intake in satiated and fasted male and female rats. PF-5190457 effect on food intake in satiated (A) and fasted (B) male and female rats 1 hour post-injection relative to baseline. PF-6870961 reduced food intake in satiated (C) and fasted (D) male and female rats 1 hour post-injection. JMV2959 reduced food intake in satiated (E) but not fasted (F) male and female rats 1 hour post-treatment. (G) Structure of JMV2959, PF-5190457, and PF-6870961 included for reference. Data represent mean ± S.E.M. *$P < 0.05$, **$P < 0.01$, difference from vehicle. $n = 10$, ○ = male rats, ▲ = female rats.
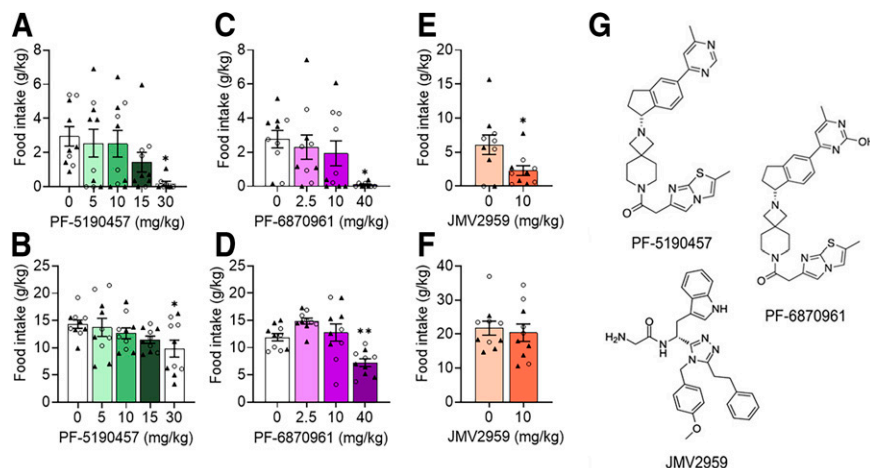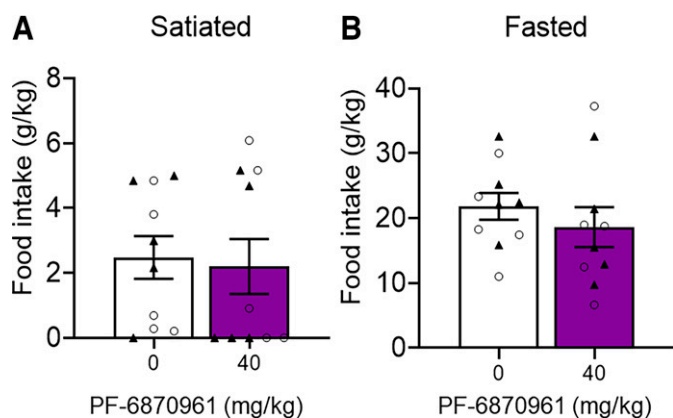
Fig. 5. Lack of effect of PF-6870961 on food intake in satiated and fasted male and female GHSR KO rats. PF-6870961 (40 mg/kg) vs. vehicle effect on food intake in satiated (A) and fasted (B) male and female rats 1 hour post-injection. Data represent mean ± S.E.M. p = ns, difference from vehicle. n = 10, ○ = male rats, ▲ = female rats.

TABLE 3
Baseline characteristics of participants in analysis of plasma concentrations of PF-5190457 and PF-6870961

Sample Size	$N = 12$
Sex, N (%)	
Male	11 (91.7)
Female	1 (8.3)
Race, N (%)	
African American	11 (91.7)
White	1 (8.3)
Smoking Status, N (%)	
Smoking	9 (75.0)
Nonsmoking	3 (25.0)
BMI in kg/m^2 (Mean ± S.E.M.)	26.9 ± 1.3
Education in Years (Mean ± S.E.M.)	12.1 ± 1.0
Age in Years (Mean ± S.E.M.)	40 ± 3.8
90-Day DDD[a] (Mean ± S.E.M.)	11.3 ± 3.8

BMI, body mass index; DDD, drinks per drinking day.
[a]From 90-day Timeline Followback (TLFB).

TMD5 movement relative to TMD3) abolished constitutive β-arrestin signaling as well as signaling via other GHSR1a-coupled pathways (Mokrosiński et al., 2012). Our findings therefore add potential structure-activity relationship insight given that the only structural difference between parent and metabolite compounds is the addition of a hydroxyl group on the piperidine ring, yet the effective inhibitory concentration for the metabolite is much lower than the concentration required for 50% occupancy of the receptor. This observation suggests that the metabolite may have a higher receptor reserve than the parent compound in the case of inverse agonism of GHSR1a-coupled β-arrestin signaling. Although further research is needed, this may be a noteworthy finding for the future design of GHSR1a inverse agonists with reduced tachyphylaxis due to β-arrestin–induced GHSR1a internalization or for biased inverse agonism of β-arrestin–coupled signaling pathways. Recently published observations of the binding mechanism of PF-5190457 suggest that the parent moiety hydroxylated on the metabolite interacts with amino acid residues on TMD3 and ECL2 via hydrophobic interactions (Qin et al., 2022), making it possible that the metabolite forms hydrogen bonds in this region that confer biased inverse agonism of β-arrestin recruitment, such as through disrupted flexibility of ECL2. Collectively, we have found that PF-5190457 and its metabolite are more potent inhibitors of GHRS1a-induced β-arrestin recruitment in comparison with LEAP-2. Future studies should compare inhibitory potency of these compounds at GHSR1a-coupled G$_{i/o}$ or G$_{12/13}$ pathways.

To determine whether PF-6870961 demonstrated an in vivo effect, we evaluated the acute effect of both parent and metabolite compounds on food intake in male and female rats. Ghrelin can influence food intake by binding to GHSR1a expressed on hypothalamic neurons that stimulate the production of orexin or by binding to GHSR1a expressed on vagal afferent neurons in the stomach (Al Massadi et al., 2019). We found that both parent and metabolite compounds dose dependently inhibited food intake in fed (rats that were not food restricted) and fasting (food withheld overnight) conditions. As expected, baseline food intake was higher in the fasted condition. Notably, the widely used prototype GHSR1a antagonist, JMV2959, did not significantly inhibit food intake in the

fasted condition but did in the satiated condition. This could be due to JMV2959 only acting as an antagonist at the GHSR1a as opposed to the inverse agonist activity observed with PF-5190457 and PF-6870961. Moreover, increased competition for GHSR1a could be expected under fasting conditions, when endogenous ghrelin is secreted into the peripheral circulation, and may be why no effect of JMV2959 on food intake was observed under fasted conditions. We did not have an a priori hypothesis that the activity of PF-5190457 and PF-6870961 would differ by sex and therefore did not power our experimental groups accordingly. Analyzing the data via a two-way ANOVA evaluating a main effect of *sex*, *dose*, and *sex × dose* interaction effect identified no significant main effect of sex; thus, our analysis was simplified to evaluate only a main effect of treatment. However, because our experiment was likely underpowered to detect an effect of sex on PF-5190457 or PF-6870961 activity, future experiments with larger sample sizes should be performed to more conclusively determine whether the parent and/or metabolite compound have sexually dimorphic efficacy.

Our results suggest that when PF-5190457 is administered to humans, its effects on the receptor would possibly reflect the combined effects of PF-5190457 and its metabolite PF-6870961. This is consistent with our results in rats that preliminarily demonstrated an in vivo effect of PF-6870961. The time-concentration profile of PF-5190457 and PF-6870961 in the plasma in humans indicate that the metabolite circulates at approximately 25% of the concentration of the parent compound, at least in humans. The majority of our sample were male participants, and all of them met criteria for heavy drinking via 90-day Timeline Followback data. Therefore, the metabolism of PF-5190457 should also be evaluated in a sample with larger representation of females as well as lower alcohol consumption to determine whether production of the PF-6870961 metabolite occurs to a different extent in either males or individuals with heavy alcohol drinking. In our phase 1b human study of PF-5190457, we identified an overall effect of PF-5190457 dose on GFCQ-S self-reported food craving after food cue exposure (Adusumalli et al., 2019a,b; Farokhnia et al., 2020; Lee et al., 2020a,b; Sulima et al., 2021). Specifically, PF-5190457 was significantly associated with lower self-reported GFCQ-S craving. We therefore set out in this manuscript to determine whether there was a relationship between
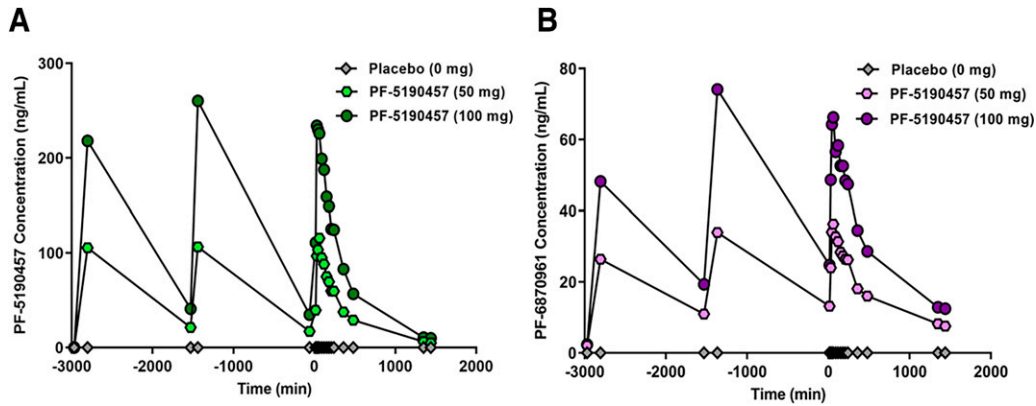
Fig. 6. Time concentration profile of plasma PF-5190457 and PF-6870961 levels in humans after repeated administrations of PF-5190457. Geometric mean plasma concentration-time pharmacokinetic profile of (A) the parent drug PF-5190457 and (B) the metabolite PF-6870961 after repeated dosing of PF-5190457 (0 mg, 50 mg, and 100 mg twice daily) in our placebo-controlled phase 1b human laboratory study in male and female individuals with heavy alcohol drinking. Dosing phase: −3000 to 0 minutes; alcohol session phase: 0 to 1440 minutes. $n = 14$. *Note: The Y-axis of (B) is expanded to show more detail.*

plasma concentrations of PF-5190457 or PF-6870961 and GFCQ-S scores since individual differences in metabolism can lead to varying concentrations of these compounds. Our preliminary analysis of the relationship between PF-5190457 or metabolite concentrations and self-reported food craving in humans revealed no correlation between these variables, but future experiments designed to compare the relationship between metabolite concentrations and food craving would allow for more powerful statistical modeling and adjustment for factors such as age, sex, etc. that may currently be washing out any existing relationship between PF-5190457 and PF-6870961 concentration and food craving. Future studies should directly compare the inhibitory potency of PF-5190457 and PF-6870961 on food intake and assess the potency of both

PF-5190457 and its metabolite administered together at expected relative concentrations. Moreover, here we only assessed the in vivo effects of PF-5190457 and PF-6870961 after acute administration, so future studies should compare the in vivo effects of both parent and metabolite compounds after chronic administration.

Following up on the previous work conducted by our laboratories (Adusumalli et al., 2019a,b; Farokhnia et al., 2020; Lee et al., 2020a,b; Sulima et al., 2021) and other groups (Kung et al., 2012; Bhattacharya et al., 2014; Kong et al., 2016; Qin et al., 2022), we expand our understanding of the pharmacological activity of PF-5190457 by demonstrating that its major hydroxy metabolite binds to GHSR1a and displays biased inverse agonism of GHSR1a-induced
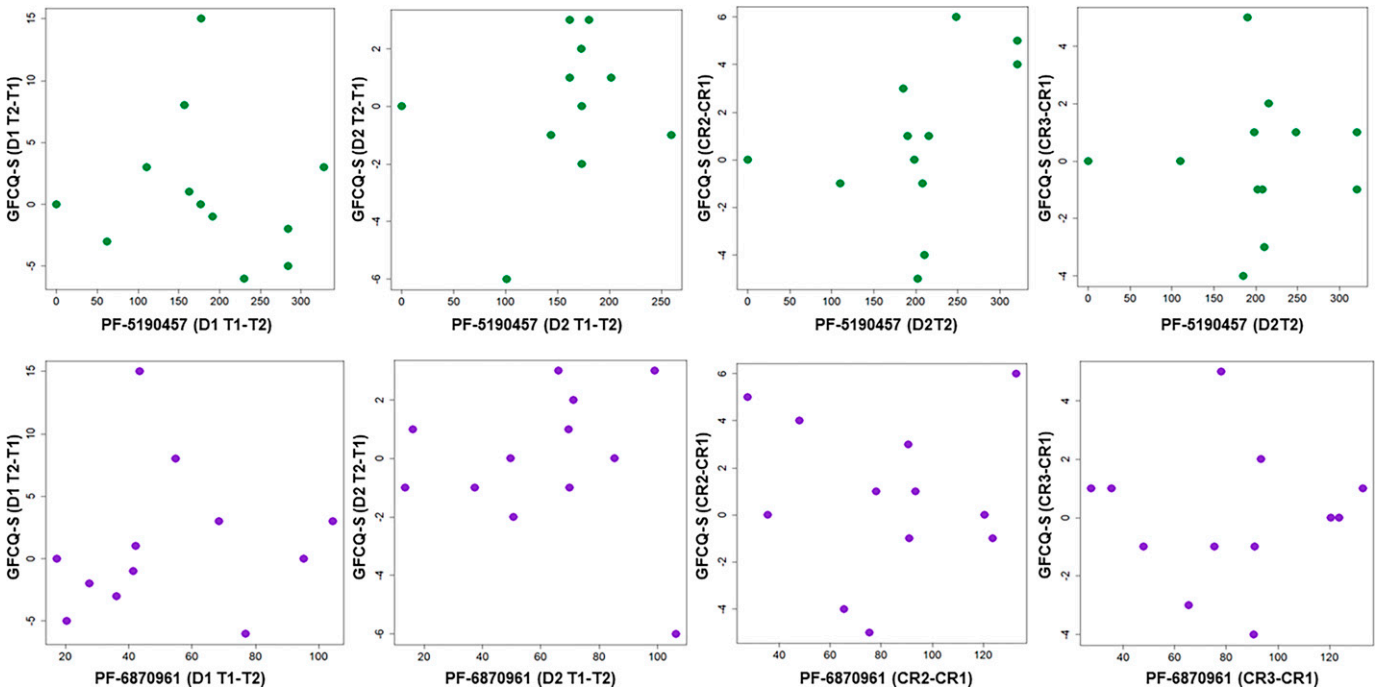

Fig. 7. Scatterplots of self-reported food craving vs. PF-5190457 or PF-6870961 plasma concentration in humans. Scatterplots depicting PF-5190457 (ng/ml) (top, green) and PF-6870961 (ng/ml) (bottom, purple) vs. GFCQ-S food craving measures during visit 3 (where subjects received 100 mg twice daily PF-5190457). $n = 12$. CR, cue reactivity.

TABLE 4
Correlations between self-reported food craving and PF-5190456 and PF-6870961 plasma concentration

Compound	Blood Draw Timepoint		GFCQ-S Timepoint	Pearson Correlation[a]	P Value	Sample Size (N)
PF-5190457						
	Day 1: T2 − T1	vs.	Day 1: T2 − T1	−0.116	0.719	12
	Day 2: T2 − T1	vs.	Day 2: T2 − T1	0.153	0.635	12
	Day 2 T2	vs.	Day 2: CR2 − CR1	0.431	0.162	12
	Day 2 T2	vs.	Day 2: CR3 − CR1	0.022	0.945	12
PF-6870961						
	Day 1: T2 − T1	vs.	Day 1: T2 − T1	0.112	0.728	12
	Day 2: T2 − T1	vs.	Day 2: T2 − T1	−0.095	0.768	12
	Day 2 T2	vs.	Day 2: CR2 − CR1	−0.015	0.963	12
	Day 2 T2	vs.	Day 2: CR3 − CR1	0.000	1.000	12

CR, cue reactivity.
[a]Pearson correlation values calculated between individual metabolite concentrations and GFCQ-S scores at different time points during visit 3 (subjects received 100 mg twice daily PF-5190457).

β-arrestin signaling. We demonstrate that both PF-5190457 and PF-6870961 significantly inhibited food intake in rats at similar doses, indicating an in vivo effect of the metabolite. We further demonstrated that the effects of this recently discovered metabolite, PF-6870961, on food intake are unequivocally mediated by GHSR1a, given the lack of similar effects in an experiment in rats lacking the receptor. Our findings presently suggest that future studies using PF-5190457 should consider additional activity due to formation of the active hydroxy metabolite PF-6870961 and are relevant for future spiro-azetidino-piperidine leads targeting GHSR1a that may undergo metabolic routes similar to PF-5190457.

Authorship Contributions

Participated in research design: Deschaine, Akhlaghi, Hougland, Koob, Vendruscolo, Holst, Leggio.

Conducted experiments: Hedegaard, Pince, Moose, Stock, Adusumalli.

Contributed new reagents or analytic tools: Sulima, Rice.

Performed data analysis: Deschaine, Hedegaard, Pince, Farokhnia, Stock, Adusumalli.

Wrote or contributed to the writing of the manuscript: Deschaine, Pince, Farokhnia, Moose, Stock, Hougland, Vendruscolo, Holst, Leggio.

References

Adusumalli S, Jamwal R, Leggio L, and Akhlaghi F (2019a) Development and validation of an assay for a novel ghrelin receptor inverse agonist PF-5190457 and its major hydroxy metabolite (PF-6870961) by LC-MS/MS in human plasma. *J Chromatogr B Analyt Technol Biomed Life Sci* **1130–1131**:121820.
Adusumalli S, Jamwal R, Obach RS, Ryder TF, Leggio L, and Akhlaghi F (2019b) Role of molybdenum-containing enzymes in the biotransformation of the novel ghrelin receptor inverse agonist PF-5190457: a reverse translational bed-to-bench approach. *Drug Metab Dispos* **47**:874–882.
Al Massadi O, Nogueiras R, Dieguez C, and Girault JA (2019) Ghrelin and food reward. *Neuropharmacology* **148**:131–138.
Bhattacharya SK, Andrews K, Beveridge R, Cameron KO, Chen C, Dunn M, Fernando D, Gao H, Hepworth D, Jackson VM, et al. (2014) Discovery of PF-5190457, a potent, selective, and orally bioavailable ghrelin receptor inverse agonist clinical candidate. *ACS Med Chem Lett* **5**:474–479.
Darling JE, Zhao F, Loftus RJ, Patton LM, Gibbs RA, and Hougland JL (2015) Structure-activity analysis of human ghrelin O-acyltransferase reveals chemical determinants of ghrelin selectivity and acyl group recognition. *Biochemistry* **54**:1100–1110.
Denney WS, Sonnenberg GE, Carvajal-Gonzalez S, Tuthill T, and Jackson VM (2017) Pharmacokinetics and pharmacodynamics of PF-05190457: the first oral ghrelin receptor inverse agonist to be profiled in healthy subjects. *Br J Clin Pharmacol* **83**:326–338.
Deschaine SL and Leggio L (2022) From "hunger hormone" to "it's complicated": ghrelin beyond feeding control. *Physiology (Bethesda)* **37**:5–15.
Farokhnia M, Faulkner ML, Piacentino D, Lee MR, and Leggio L (2019) Ghrelin: from a gut hormone to a potential therapeutic target for alcohol use disorder. *Physiol Behav* **204**:49–57.
Farokhnia M, Grodin EN, Lee MR, Oot EN, Blackburn AN, Stangl BL, Schwandt ML, Farinelli LA, Momenan R, Ramchandani VA, et al. (2018) Exogenous ghrelin administration increases alcohol self-administration and modulates brain functional activity in heavy-drinking alcohol-dependent individuals. *Mol Psychiatry* **23**:2029–2038.
Farokhnia M, Portelli J, Lee MR, McDiarmid GR, Munjal V, Abshire KM, Battista JT, Browning BD, Deschaine SL, Akhlaghi F, et al. (2020) Effects of exogenous ghrelin administration and ghrelin receptor blockade, in combination with alcohol, on peripheral inflammatory markers in heavy-drinking individuals: results from two human laboratory studies. *Brain Res* **1740**:146851.
Ge X, Yang H, Bednarek MA, Galon-Tilleman H, Chen P, Chen M, Lichtman JS, Wang Y, Dalmas O, Yin Y, et al. (2018) LEAP2 is an endogenous antagonist of the ghrelin receptor. *Cell Metab* **27**:461–469.e6.
Gomez JL and Ryabinin AE (2014) The effects of ghrelin antagonists [D-Lys(3)]-GHRP-6 or JMV2959 on ethanol, water, and food intake in C57BL/6J mice. *Alcohol Clin Exp Res* **38**:2436–2444.
Hedegaard MA and Holst B (2020) The complex signaling pathways of the ghrelin receptor. *Endocrinology* **161**:bqaa020.
Holst B, Cygankiewicz A, Jensen TH, Ankersen M, and Schwartz TW (2003) High constitutive signaling of the ghrelin receptor–identification of a potent inverse agonist. *Mol Endocrinol* **17**:2201–2210.
Jerlhag E, Egecioglu E, Landgren S, Salomé N, Heilig M, Moechars D, Datta R, Perrissoud D, Dickson SL, and Engel JA (2009) Requirement of central ghrelin signaling for alcohol reward. *Proc Natl Acad Sci USA* **106**:11318–11323.
Kaur S and Ryabinin AE (2010) Ghrelin receptor antagonism decreases alcohol consumption and activation of perioculomotor urocortin-containing neurons. *Alcohol Clin Exp Res* **34**:1525–1534.
Kong J, Chuddy J, Stock IA, Loria PM, Straub SV, Vage C, Cameron KO, Bhattacharya SK, Lapham K, McClure KF, et al. (2016) Pharmacological characterization of the first in class clinical candidate PF-05190457: a selective ghrelin receptor competitive antagonist with inverse agonism that increases vagal afferent firing and glucose-dependent insulin secretion ex vivo. *Br J Pharmacol* **173**:1452–1464.
Kung DW, Coffey SB, Jones RM, Cabral S, Jiao W, Fichtner M, Carpino PA, Rose CR, Hank RF, Lopaze MG, et al. (2012) Identification of spirocyclic piperidine-azetidine inverse agonists of the ghrelin receptor. *Bioorg Med Chem Lett* **22**:4281–4287.
Landgren S, Simms JA, Hyytiä P, Engel JA, Bartlett SE, and Jerlhag E (2012) Ghrelin receptor (GHS-R1A) antagonism suppresses both operant alcohol self-administration and high alcohol consumption in rats. *Addict Biol* **17**:86–94.
Lee MR, Farokhnia M, Cobbina E, Saravanakumar A, Li X, Battista JT, Farinelli LA, Akhlaghi F, and Leggio L (2020a) Endocrine effects of the novel ghrelin receptor inverse agonist PF-5190457: results from a placebo-controlled human laboratory alcohol co-administration study in heavy drinkers. *Neuropharmacology* **170**:107788.
Lee MR, Tapocik JD, Ghareeb M, Schwandt ML, Dias AA, Le AN, Cobbina E, Farinelli LA, Bouhlal S, Farokhnia M, et al. (2020b) The novel ghrelin receptor inverse agonist PF-5190457 administered with alcohol: preclinical safety experiments and a phase 1b human laboratory study. *Mol Psychiatry* **25**:461–475.
Leggio L, Zywiak WH, Fricchione SR, Edwards SM, de la Monte SM, Swift RM, and Kenna GA (2014) Intravenous ghrelin administration increases alcohol craving in alcohol-dependent heavy drinkers: a preliminary investigation. *Biol Psychiatry* **76**:734–741.
McGovern-Gooch KR, Mahajani NS, Garagozzo A, Schramm AJ, Hannah LG, Sieburg MA, Chisholm JD, and Hougland JL (2017) Synthetic triterpenoid inhibition of human ghrelin O-acyltransferase: the involvement of a functionally required cysteine provides mechanistic insight into ghrelin acylation. *Biochemistry* **56**:919–931.

Mokrosiński J, Frimurer TM, Sivertsen B, Schwartz TW, and Holst B (2012) Modulation of constitutive activity and signaling bias of the ghrelin receptor by conformational constraint in the second extracellular loop. *J Biol Chem* **287**:33488–33502.

Morris LS, Voon V, and Leggio L (2018) Stress, motivation, and the gut-brain axis: a focus on the ghrelin system and alcohol use disorder. *Alcohol Clin Exp Res* **42**:1378–1389.

Moulin A, Brunel L, Boeglin D, Demange L, Ryan J, M'Kadmi C, Denoyelle S, Martinez J, and Fehrentz JA (2013) The 1,2,4-triazole as a scaffold for the design of ghrelin receptor ligands: development of JMV 2959, a potent antagonist. *Amino Acids* **44**:301–314.

Qin J, Cai Y, Xu Z, Ming Q, Ji SY, Wu C, Zhang H, Mao C, Shen DD, Hirata K, et al. (2022) Molecular mechanism of agonism and inverse agonism in ghrelin receptor. *Nat Commun* **13**:300.

R Core Team (2022) *R: A Language and Environment for Statistical Computing*, R Foundation for Statistical Computing, Vienna, Austria.

Riddles PW, Blakeley RL, and Zerner B (1979) Ellman's reagent: 5,5'-dithiobis(2-nitrobenzoic acid)–a reexamination. *Anal Biochem* **94**:75–81.

Sieburg MA, Cleverdon ER, and Hougland JL (2019) Biochemical assays for ghrelin acylation and inhibition of ghrelin O-acyltransferase. *Methods Mol Biol* **2009**:227–241.

Spiess K, Bagger SO, Torz LJ, Jensen KHR, Walser AL, Kvam JM, Møgelmose AK, Daugvilaite V, Junnila RK, Hjortø GM, et al. (2019) Arrestin-independent constitutive endocytosis of GPR125/ADGRA3. *Ann N Y Acad Sci* **1456**:186–199.

Suchankova P, Steensland P, Fredriksson I, Engel JA, and Jerlhag E (2013) Ghrelin receptor (GHS-R1A) antagonism suppresses both alcohol consumption and the alcohol deprivation effect in rats following long-term voluntary alcohol consumption. *PLoS One* **8**:e71284.

Sulima A, Akhlaghi F, Leggio L, and Rice KC (2021) Synthesis of PF-6870961, a major hydroxy metabolite of the novel ghrelin receptor inverse agonist PF-5190457. *Bioorg Med Chem* **50**:116465.

Yanagi S, Sato T, Kangawa K, and Nakazato M (2018) The homeostatic force of ghrelin. *Cell Metab* **27**:786–804.

You ZB, Galaj E, Alén F, Wang B, Bi GH, Moore AR, Buck T, Crissman M, Pari S, Xi ZX, et al. (2022) Involvement of the ghrelin system in the maintenance and reinstatement of cocaine-motivated behaviors: a role of adrenergic action at peripheral β1 receptors. *Neuropsychopharmacology* **47**:1449–1460.

Zallar LJ, Beurmann S, Tunstall BJ, Fraser CM, Koob GF, Vendruscolo LF, and Leggio L (2019a) Ghrelin receptor deletion reduces binge-like alcohol drinking in rats. *J Neuroendocrinol* **31**:e12663.

Zallar LJ, Farokhnia M, Tunstall BJ, Vendruscolo LF, and Leggio L (2017) The role of the ghrelin system in drug addiction. *Int Rev Neurobiol* **136**:89–119.

Zallar LJ, Tunstall BJ, Richie CT, Zhang YJ, You ZB, Gardner EL, Heilig M, Pickel J, Koob GF, Vendruscolo LF, et al. (2019b) Development and initial characterization of a novel ghrelin receptor CRISPR/Cas9 knockout Wistar rat model. *Int J Obes* **43**:344–354.

Address correspondence to: Dr. Lorenzo Leggio, National Institute on Drug Abuse and National Institute on Alcohol Abuse and Alcoholism, National Institutes of Health, Biomedical Research Center, Room 04A511, 251 Bayview Boulevard, Baltimore, MD 21224. E-mail: lorenzo.leggio@nih.gov

Initial pharmacological characterization of a major hydroxymetabolite of PF-5190457: inverse agonist/antagonist activity of PF-6870961 at the ghrelin receptor

Sara L. Deschaine[1,2], Morten A. Hedegaard[3], Claire L. Pince[1,4], Mehdi Farokhnia[1,5], Jacob E. Moose[6], Ingrid A. Stock[7], Sravani Adusumalli[8], Fatemeh Akhlaghi[8], James L. Hougland[6,9,10], Agnieszka Sulima[11,12], Kenner C. Rice[11,12], George F. Koob[4], Leandro F. Vendruscolo[4], Birgitte Holst[3], Lorenzo Leggio[1,11,13,14]*

Supplementary Appendix S1. Inclusion and Exclusion Criteria

Inclusion criteria:

- o Males or females 21-65 years old (inclusive)

- o Heavy drinking (least 21 drinks per week for men or at least 14 drinks for women on average via the 90-day timeline follow-back done at screening)

- o Negative urine drug screen and good health as confirmed by medical history, physical examination, electrocardiogram (EKG), blood/urine lab tests

- o Female subjects must be of non-childbearing potential as defined by at least one of the following criteria:

   1. Females 45 – 65 years old, who are menopausal, defined as follows:

      Females who are between 45 – 55 years old will be considered menopausal if they satisfy all the following three requirements during screening:

      - ▪ In amenorrhea, defined as absence of menstruation for the previous 12 months
      - ▪ Negative urine pregnancy test
      - ▪ Serum follicle-stimulating hormone concentration within the laboratory's reference range for postmenopausal females

Females who are between 56 – 65 years old are considered menopausal if they are in amenorrhea, defined as absence of menstruation for the previous 12 months before screening

OR

2. Females 21-65 years old, who have a documented hysterectomy and/or bilateral oophorectomy

All other female subjects (including females with tubal ligations and females that do not have a documented hysterectomy) are considered to be of childbearing potential

o Male subjects must use one of the following methods of contraception from the first dose of study medication and until 28 days after dosing:

   a. Abstinence

   b. A condom AND one of the following:

      i. Vasectomy for more than 6 months

      ii. Female partner who meets one of the following conditions

      a. Has had a tubal ligation, hysterectomy, or bilateral oophorectomy

      b. Is post-menopausal

      c. Uses one of the following forms of contraception

         • Copper or hormonal containing intrauterine device

         • Spermicidal foam/gel/film/cream/suppository

         • Diaphragm with spermicide

         • Oral contraceptive

         • Injectable progesterone

         • Subdermal implant

Exclusion criteria:

• Interest in receiving treatment for heavy drinking

- Current Diagnostic and Statistical Manual of Mental Disorders-IV (DSM-IV) diagnosis (based on structured clinical interview for DSM-IV) of substance dependence (other than alcohol and/or nicotine);

- DSM-IV Axis I criteria for a lifetime diagnosis of schizophrenia, bipolar disorder, or other psychoses

- Active illness within the past 6 months of the screening visit that meet the DSM-IV criteria for a diagnosis of major depressive disorder or anxiety disorder; any history of attempted suicide. Clinically significant medical abnormalities (e.g., unstable hypertension, clinically significant EKG abnormalities, Creatinine ≥ 2 mg/dL, liver cirrhosis, aspartate aminotransferase or alanine transaminase > 3x the upper normal limit, hemoglobin <10.5 g/dl)

- Heart rate >100 at screening on two separate measurements

- Body Mass Index (BMI) ≤ 18.5 or anorexia

- BMI ≥ 35 kg/m^2

- Exclusionary Medications:

- Naltrexone, acamprosate, alcohol dehydrogenase inhibitors, topiramate, gabapentin, ondansetron, benzodiazepines, beta-blockers, H2-blockers, and alpha-1 blockers, baclofen and barbiturates as well as hormone replacement therapy; medications and dietary/herbal supplements (e.g. St. John's wort) that interact with Cytochrome P450 3A4. All medications in the previous sentence are exclusionary if taken within 2 weeks of study medication administration.

- PF-5190457 is a substrate for P-glycoproteins (P-gp or encoded by ABCB1 gene) based on information from in vitro or animal models. Patients that are required to take the following inhibitors and inducers of P-gp are excluded unless the subject stops taking these agents for 2 weeks for P-gp inhibitors or 6 weeks for P-gp inducers before study medication administration:

i. *Inhibitors*: Amiodarone, azithromycin, captopril, carvedilol, clarithromycin, conivaptan, cyclosporine, diltiazem, dronedarone, erythromycin, felodipine, itraconazole, ketoconazole, lopinavir and ritonavir, quercetin, quinidine, ranolazine, verapamil

ii. *Inducers*: Avasimibe, carbamazepine, phenytoin, rifampin, St John's wort, tipranavir/ritonavir

[From Drug Development and Drug Interactions: Table of Substrates, Inhibitors and Inducers, table 12, from http://www.fda.gov/Drugs/DevelopmentApprovalProcess/DevelopmentResources/DrugInteractionsLabeling/ucm093664.htm#substrates]

- History of epilepsy or alcohol-related seizures

- Patients who have diabetes and/or are treated with any drug with glucose lowering properties such as sulfonylurea, insulin, metformin, thiazolidinediones, dipeptidyl peptidase-4 inhibitors, or glucagon-like peptide-1 agonists (due to the glucose-lowering properties of PF-5190457 observed in healthy volunteers)

- History of alcohol-induced flushing reactions

- Clinically significant alcohol withdrawal symptoms, as assessed by a Clinical Institute Withdrawal Assessment of Alcohol Scale Revised score > 8 at screening

- Any other reason or clinical condition for which the principal investigator or the medical advisory investigator consider unsafe for a possible participant to participate in this study

Supplementary Table 1: % Inhibition of Off-Target Binding and Enzymatic Activity of PF-6870961

Target	Radioligand	% Inhibition at 100 nM	% Inhibition at 10000 nM
Binding			
A_1 (h)	Antagonist	-8.5	-5.3
A_{2A} (h)	Agonist	1.3	5.8
A_{2B} (h)	Antagonist	-1.3	-30.2
A_3 (h)	Agonist	-7.6	-5.6
α_1 (Non-selective)	Antagonist	1.9	7.9
α_2 (Non-selective)	Antagonist	-5.2	1.8
β_1 (h)	Agonist	7.2	5.7
AT_1 (h)	Antagonist	-4.5	0.7
AT_2 (h)	Agonist	2.4	1.7
BZD	Agonist	-19.6	-17.6
B_2	Agonist	-2.9	1.6
CB_1	Agonist	-6.4	-2.8
CB_2	Agonist	2.9	0.7
CCK_1	Agonist	9.5	13.7
CCK_2	Agonist	-0.6	-2.0
CRF_1	Agonist	-1.1	-3.3
$D_{4.4}$	Antagonist	13.1	43.5
ET_A	Agonist	-6.6	-4.0
ET_B	Agonist	-11.0	-26.0
$GABA_{A1}$	Agonist	-7.6	6.9
$GABA_{B(1b)}$	Antagonist	-13.9	-1.1
GAL_1	Agonist	-3.2	-0.4
GAL_2	Agonist	-0.7	-2.1
AMPA	Agonist	-8.1	-11.4
kainate	Agonist	3.1	37.9
NMDA	Antagonist	2.2	1.1
mGluR1	Agonist	-11.6	7.3
mGluR5	Agonist	-1.6	-8.0
Glycine (strychnine-sensitive)	Antagonist	15.9	1.6
Glycine (strychnine-insensitive)	Antagonist	-2.9	-6.7
H_1	Antagonist	3.4	1.5
H_2	Antagonist	-1.5	10.7
H_3	Agonist	-11.4	9.1
$CysLT_1$ (LTD_4)	Agonist	-1.5	2.5
M (non-selective)	Antagonist	8.4	39.8
M_1	Antagonist	6.4	19.2
M_2	Antagonist	-18.1	9.1
M_3	Antagonist	-0.4	4.8
NK_1	Agonist	-14.6	8.1
NK_2	Agonist	-7.4	14.5
NK_3	Antagonist	7.6	13.3
N neuronal $\alpha4\beta2$	Antagonist	1.6	0.2
N neuronal $\alpha7$	Antagonist	0.5	30.4
N muscle type	Antagonist	-8.0	3.8
δ (DOP)	Agonist	10.0	10.7
κ (KOP)	Agonist	-9.9	8.5
μ (MOP)	Agonist	1.7	12.8
Oxytocin	Agonist	-0.5	4.3

NOP	Agonist	5.8	0.8
PAF	Agonist	1.1	6.6
PCP	Antagonist	3.8	1.5
GR	Agonist	7.3	-9.8
ER (non-selective)	Agonist	4.9	-3.6
AR	Agonist	11.3	-4.1
TRH_1	Agonist	-2.9	-8.4
$VPAC_2$	Agonist	-6.3	-12.1
$VPAC_1$	Agonist	-8.1	-10.4
V_{1a}	Agonist	7.8	5.0
V_{1b}	Agonist	-1.7	10.9
Ca+2 channel (L, dihydropyridine site)	Antagonist	-31.5	-8.6
Ca +2 channel (L, diltiazem site)	Antagonist	-1.5	-8.5
Ca^{2+} channel (N)	Antagonist	2.2	2.8
K_{ATP} channel	Antagonist	6.6	-1.3
SK_{ca} channel	Antagonist	-8.8	-6.5
Na^+ channel (site 2)	Antagonist	11.6	8.2
Enzyme			
Choline Acetyl Transferase		-4.0	46.4
TXA_2 Synthetase		-1.1	15.2
Constitutive NOS (endothelial)		-17.7	30.7
Acetylcholinesterase (h)		5.8	36.3
MAO-A		-0.1	2.9
MAO-B		-24.0	-14.6

Supplementary Table 2: %Inhibition of Dopamine, Serotonin, and Opioid Receptors and Related Transporters

Target	Radioligand	% Inhibition at 100 nM	% Inhibition at 10 μM
5HT1A	[^{3}H]8OH-DPAT	0.85 ± 4.01%	14.71 ± 0.99%
5HT2A	[^{3}H]5-HT	14 ± 14%	0.50 ± 16.79%
5HT2C	[^{3}H]5-HT	3.9 ± 5.6%	18.16 ± 0.09%
DA D1	[^{3}H]SCH 23390	-4.3 ± 5.1%	-7.0 ± 6.6%
DA D2	[^{3}H]YM-09151-2	0.89 ± 6.15%	9.58 ± 0.31%
DA D3	[^{3}H]YM-09151-2	-3.0 ± 5.4%	10.57 ± 0.44%
DA D4.4	[^{3}H]YM-09151-2	-2.2 ± 6.2%	22.3 ± 1.5%
δ (DOP)	[^{3}H]DPDPE	-2.7 ± 1.5%	3.36 ± 0.24%
κ (KOP)	[^{3}H]U69,593	5.7 ± 3.2%	11.8 ± 4.1%
μ (MOP)	[^{3}H]DAMGO	11.5 ± 4.3%	26.1 ± 3.7%
DAT	[^{125}I]RTI-55	16.1 ± 1.7%	17.5 ± 3.0%
SERT	[^{125}I]RTI-55	5.07 ± 0.91%	7.9 ± 2.4%
NET	[^{125}I]RTI-55	14.22 ± 0.58%	23.8 ± 1.5%

Data are expressed as the % inhibition of specific control binding. Numbers represent the means ± range from two independent experiments, each conducted with at least triplicate determinations. Negative inhibition values indicate that more specific binding was measured in the presence of PF-6870961than under control conditions

Supplementary Table 3: Mean Plasma Concentration of PF-5190457 and PF-6870961

	50 mg BID PF-5190457		100 mg BID PF-6870961	
	PF-5190457 (ng/mL)	PF-6870961 (ng/mL)	PF-5190457 (ng/mL)	PF-6870961 (ng/mL)
Day 1				
Pre-Dose	-	2.06	-	2.34
Post-Dose	105.52	26.40	218.07	48.17
Day 2				
Pre-Dose	21.26	10.94	41.01	19.35
Post-Dose	106.57	33.92	260.34	74.13

BID = twice daily
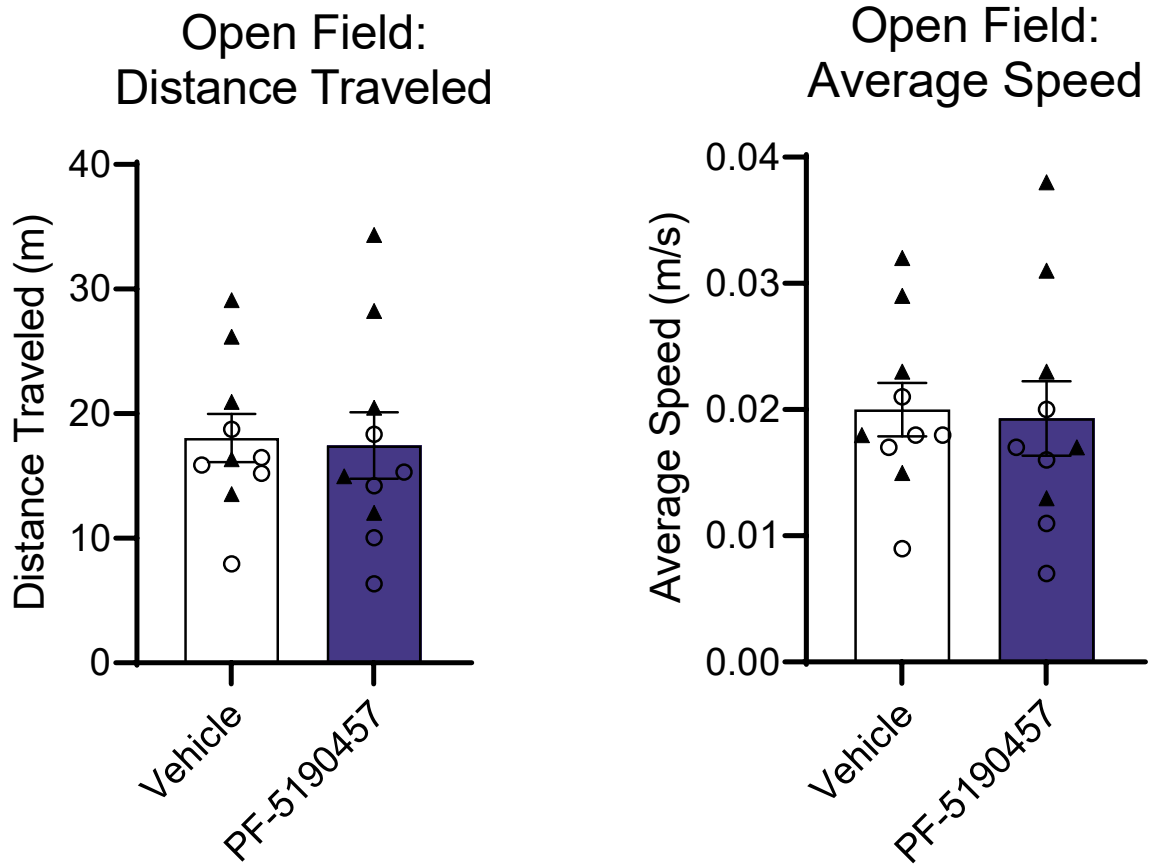
Supplementary Figure S1. PF-51904575 (30 mg/kg) had no effect on spontaneous locomotion in rats as measured by distance traveled (m) (**left**) and average speed (m/s) (**right**) in an open field test. Data are shown as mean ± S.E.M and analyzed using a two-tailed, paired t test. $n = 10$, ○ = male rats, ▲ = female rats.